

Chemistry under EUV Irradiation of H₂-CO-N₂ Gas Mixtures

Implications for Photochemistry in the Outer CSE of Evolved Stars

J.Bourgalais^{1,*}, D.V.Bekaert², A.Bacmann³, B.Marty² and N.Carrasco¹

¹ Université Versailles St-Quentin, Sorbonne Université, UPMC Univ. Paris 06, CNRS/INSU, LATMOS-IPSL, 11 boulevard d' Alembert, 78280 Guyancourt, France

² Centre de Recherches Pétrographiques et Géochimiques, CNRS, Université de Lorraine, 15 rue Notre Dame des Pauvres, BP 20, 54501 Vandoeuvre lès Nancy, France

³ Univ. Grenoble Alpes, CNRS, IPAG, 38000 Grenoble, France

Received XX XX, 20XX; accepted XX XX, 20XX

ABSTRACT

Context. CircumStellar Envelopes (CSEs) of stars are complex chemical objects for which theoretical models encounter difficulties in elaborating a comprehensive overview of the occurring chemical processes. Along with photodissociation, ion-neutral reactions and dissociative recombination might play an important role in controlling molecular growth in outer CSEs.

Aims. The aim of this work is to provide experimental insights into pathways of photochemistry-driven molecular growth within outer CSEs to draw a more complete picture of the chemical processes occurring within these molecule-rich environments. A simplified CSE environment was therefore reproduced in the laboratory through gas-phase experiments exposing relevant gas mixtures to an Extreme UltraViolet (EUV) photon source. This photochemical reactor should ultimately allow us to investigate chemical processes and their resulting products occurring under conditions akin to outer CSEs.

Methods. We used a recently developed EUV lamp coupled to the APSIS photochemical cell to irradiate CSE relevant gas mixtures of H₂, CO and N₂, at one wavelength, 73.6 nm. The detection and identification of chemical species in the photochemical reactor was achieved through in-situ mass spectrometry analysis of neutral and cationic molecules.

Results. We find that exposing CO-N₂-H₂ gas mixtures to EUV photons at 73.6 nm induces photochemical reactions that yield the formation of complex, neutral and ionic species. Our work shows that N₂H⁺ can be formed through photochemistry along with highly oxygenated ion molecules like HCO⁺ in CSE environments. We also observe neutral N-rich organic species including triazole and aromatic molecules.

Conclusions. These results confirm the suitability of our experimental setting to investigate photochemical reactions and provide fundamental insights into the mechanisms of molecular growth in the outer CSEs. Especially, this work supports a potential reaction mechanism from simple species to monocyclic system toward the formation of Nitrogenized Polycyclic aromatic hydrocarbons (NPAHs) that could occur in circumstellar environments but also in the InterStellar Medium (ISM).

Key words. Molecular processes – Astrochemistry – Methods: laboratory: molecular – Stars: circumstellar matter – Ultraviolet: stars

1. Introduction

The outermost regions of CSEs are dominated by H₂, followed in abundance by CO and N₂ (CO/H₂ ca. 1.5×10^{-4} Decin et al. (2010); N₂/H₂ ca. 2.0×10^{-4} Gobrecht et al. (2016)). Most of the molecules observed in CSEs originate from their outer, cold and sparse shells, whose study is of particular interest to improve our understanding on molecular formation/destruction processes, material recycling during stellar evolution and, more generally, macroscopic processes in astrophysics (e.g., stellar mass-loss history, wind acceleration, dust formation, nucleosynthesis). While stellar blackbody photons coming from the star play a role in the chemistry of inner CSEs (Van de Sande & Millar 2019), outer shells are photon-dominated regions exposed to interstellar UV photon flux coming from nearby stars, initiating an active chemistry with competing photochemical processes, see Agúndez et al. (2017) and references therein. The abundant UV photons photo-dissociate and photo-ionize the main species, therefore playing an important role in the formation of reactive species such as radicals and ions that will then rapidly react through ion-molecule reactions, radical chemistry and dissociative recombination, to build up the local molecular complexity (Li et al. 2013). Due to the enhanced reaction rates of ions compared to neutral species (Van Dishoeck 2014), ionic chemistry would dominate molecular growth processes (Li et al. 2014).

*jeremy.bourgalais@latmos.ipsl.fr

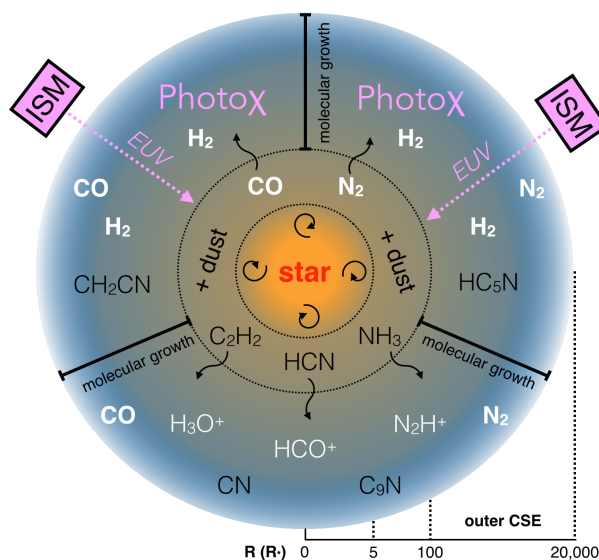


Fig. 1. Schematic structure of the CSE for an O-rich AGB star, adapted and modified from Li et al. (2016). The region of the CSE that is tentatively reproduced with the present experimental setting corresponds to the outer CSE (ca. 100 to 20,000 R^* , where R^* is the radius of the central star), where photochemical species are formed primarily by photodissociation of parental species.

Fully understanding molecular abundances from astronomical observations (Agúndez et al. 2012) requires predictive modelling of chemical processes potentially occurring within CSEs. To this end, advanced astrochemical models are developed by considering many physical regimes and extensive chemical networks (thousands of reactions among hundred species). However, only two thirds of the species observed in CSEs were found to have densities that agreed with model-derived predictions within one order of magnitude, therefore demonstrating that some important uncertainties remain regarding the gas-phase chemical kinetics in the outermost parts of CSEs. Critical experimental data are required to further constrain photodissociation and reaction rate coefficients, as well as ion-molecule reaction pathways.

In this study, we aim at setting an experiment allowing novel insights into ion-driven molecular growth processes occurring in the irradiated, outer regions of CSE. To this end, a simplified CSE environment has been reproduced in the laboratory through gas-phase experiments exposing relevant gas mixtures of H_2 , CO and N_2 , the main species in the outer CSE, to an EUV photon source tuned at 73.6 nm, therefore reaching the ionization thresholds of CO and N_2 . This work focuses on the chemical processes and resulting products formed under conditions reminiscent to outer CSEs illustrated in Figure 1. In the following sections, we report the positive detection of neutral and ion species that have, for part of them, already been observed in CSEs. Then, we discuss their potential implications for the chemical composition of circumstellar media.

2. Experimental Method

2.1. An EUV Source Coupled Windowless with a Photochemical Reactor

EUV irradiation of H_2 - CO - N_2 gas mixtures as carried out in the APSIS reactor already used in the past for UV photochemical experiments simulating complex, diluted and reactive environments akin to planetary upper atmospheres (Carrasco et al. 2013; Peng et al. 2013; Bourgalais et al. 2019).

The reactor is a stainless steel chamber with a volume of 5,000 cm^3 which is pumped down to $\sim 3 \times 10^{-7}$ mbar and baked at 60°C, before each experiment, in order to minimize residual gas traces in the chamber. The reactive gas mixtures are flowed continuously into the reactor by using mass flow controller with a total flow rate of 6 sccm (standard centimeter cube per minute) resulting in a partial pressure of ca. 0.33 mbar. The experiments are performed at a total pressure of ca. 0.9 mbar due to the injection of neon coming from the UV source and at room temperature.

The gas mixtures are irradiated at 73.6 nm (16.8 eV) by using a neon gas-discharge lamp which is coupled windowless to the photochemical reactor. This EUV source has been described in Tigrine et al. (2016) and used in Bourgalais et al. (2019). A quarter inch tube is used to flow a continuous 12 sccm of neon ensuring a photon flux of $\sim 10^{14}$ $ph\ s^{-1}\ cm^{-2}$ by operating the discharge lamp with a power of 70 W and a frequency of 2.6 GHz. The tube is slid into the middle of the reactor in order to limit the impact of the recombination of reactive species on the walls.

In this work, the rare gas used for the VUV lamp and the other species from gas mixtures were provided by Air Liquide (purities of 99.999%, respectively). The experiments were repeated at least twice to ensure their repeatability. The relative proportions of H_2 - CO - N_2 were varied within experimental limitations inherent to the APSIS setup in order to test their respective contributions in the formation of photochemical products. Two gas mixtures have been used with different initial fractional abundances of H_2 , CO , and N_2 . The first one is a 1:1:1 mixing ratio gas mixture in order to maximize the molecular growth containing ionic hetero-atoms compounds (ie. N/O- bearing species) in the reactor. The second gas mixture aims at mimicking a H-dominated environment with a 1:0.01:0.01 mixing ratio more relevant to CSE environments.

2.2. Comparison of the Experimental Conditions with outer CSEs

H₂ plays an important role as co-reactant during ion-molecule reactions through H-transfer to form hydrogenized cations. On the other hand, photodissociation and photoionization of CO, which encloses almost all volatile carbon in outer CSEs, have an impact on carbon and nitrogen chemistry (Li et al. 2014). N₂ is the major carrier of N in outer CSEs (Li et al. 2014), where photodissociation is the primary destruction pathway that controls the abundance of N-bearing species. In the present study, the pressure in the reactor was ca. 0.9 mbar, at room temperature. Despite discrepancies between the physical parameters in the simulated (300 K, 10¹⁶ molecules cm⁻³) and astrophysical (25 K and 10⁵ molecules cm⁻³) environments, those chosen in this work are optimized to study photochemical mechanisms expected in the outer CSEs, which are driven by ion-molecule reactions that are weakly temperature-dependent and fast enough (ca. 10⁻⁹ molecules⁻¹ s⁻¹ cm³) to minimize intermolecular effects at this pressure (ca. 10⁻¹² molecules⁻¹ s⁻¹ cm³) (Hébrard et al. 2009).

In this work the mono-wavelength gas-discharge system allows to mimic the interstellar UV field irradiation of relevant gas mixtures with EUV photons which are difficult to produce in the laboratory. The mean interstellar radiation field (ISRF) flux is considered to be 10⁸ photons cm⁻² s⁻¹ between 6 and 13.6 eV (Habing 1968), but this work was performed at 16.8 eV. At this high energy stars do not contribute much, but emission by hot plasmas (coronal gas in the halo and supernova remnants) dominates the radiation field with a photons flux lower by ca. 2 to 4 orders of magnitude (Tielens 2005). An irradiation of one hour in our experiment corresponds to an irradiation on a CSE of ca. 10⁴ to 10⁶ years, taking the uncertainty in the EUV photon flux of the ISRF into account. The photons flux used in this work leads to an ionization rate in the reactor of ca. 10⁻⁶ s⁻¹ which is close to what was reported for PDR regions, ca. 10⁻⁸ s⁻¹ (Ilgner & Nelson 2006).

2.3. Mass Spectrometry Analysis

The products following the irradiation of the gas mixtures were monitored by using a quadrupole mass spectrometer (Hiden Analytical EQP 200 QMS). The tip of the QMS is set up 1 cm perpendicularly to the axis of the photon flux after the exit quartz flow tube and the gas sampling is achieved through a small pinhole of 100 microns in diameter. The mass spectrometer allows high sensitivity (< 1 ppm) in situ measurements of the gas phase composition (positive and negative ions, neutral species) (Bourgalais et al. 2019; Dubois et al. 2019).

However, due to a rapid transport of the molecules in our reactor and an electronic ionization at 70 eV with the mass spectrometer, the observation of large neutrals species remains difficult (Bourgalais et al. 2019). The neutral mass spectra are moreover complicated by the dominant signature of the reactants H₂, CO, and N₂. These species contribute actually to numerous ion peaks, both through complex fragmentation pattern by electronic impact at 70 eV in the ionization chamber of the mass spectrometer and through their isotopic natural contributions. The number of neutral photoproducts that we observe is therefore limited.

Thus, to improve the detection of neutral species, the gas flow was passed through a cold trap held at liquid nitrogen temperature (77K at atmospheric pressure) for 3 to 6 hours, therefore allowing condensable species to be concentrated (Gautier et al. 2011). At the end of each experiment, the cold trap still at liquid nitrogen temperature was exposed to high vacuum for 1 min to remove non-condensable species, before being isolated, warmed up to room temperature and open on the APSIS reactor in static mode for mass spectrometry analysis.

Mass spectra reported in this study are the average of 10 scans obtained at 2 s/uma with a channeltron-type detection, over the 1-100 amu mass range. Uncertainties are computed for each mass from the standard deviation of the 10 scans. In all the spectra presented below, signals <10 cps are considered as background noise. The reported mass spectra show the direct signals recorded without background subtraction.

3. Results and Discussion

3.1. Neutrals

The *in situ* measurement mass spectra in Figure 2 displays the abundant peaks of the initial gas mixture species H₂ ($m/z = 2$), CO and N₂ (both at $m/z = 28$, with isotopologues at m/z of 29, 30 and 31). Atomic species H, C, N and O resulting from the fragmentation of their parental molecules upon photodissociation are observed at m/z of 1, 12, 14 and 16, respectively. Peaks at m/z of 20, 21 and 22 match the isotope relative abundances of neon, which is the non reactive gas flowed continuously in the photochemical reactor. Peaks at m/z of 10 are attributed to double ionized ²⁰Ne²⁺, respectively, produced in the mass spectrometer itself by electron impact ionization at 70 eV for the detection of neutral species. Finally, peaks at m/z of 17 (OH⁺) and 18 (H₂O⁺) indicate that water is the major trace species in the reactor coming from contamination but which is present in trace amounts (mixing ratio of 10⁻³ compared to N₂). This give an estimate of the level of contamination in the system. High amounts of H₂O have been found in AGB stars, it can have an important impact for the chemistry in the envelope as an important OH radical source (González-Alfonso et al. 1998; González-Alfonso & Cernicharo 1999; Maercker et al. 2009; Neufeld et al. 2011). Thus, the presence of water vapor traces in the reactor provides a study of the impact of water vapor in surrounding AGB stars environments. Smaller signatures that could be observed below 100 counts in situ mass spectrum (Figure 3) at m/z of 32, 40 and 44, corresponds to O₂, Ar, and CO₂ respectively (residual air in the mass spectrometer) which do not interfere in the chemistry of the reactor (Carrasco et al. 2007).

Typical non-normalized gas-phase mass spectra for neutral species with a 1:1:1 mixing ratio H₂-CO-N₂ gas mixture irradiated at 73.6 nm in the APSIS chamber at a total pressure of 0.9 mbar are reported Figure 3. Neutral species detected in the spectrum obtained after 6 hours of accumulation in a cryogenic trap are compared to the *in situ* measurement following a few minutes of EUV irradiation. No detectable signal related to photochemistry is observed from direct *in situ* measurements, therefore promoting the use of a cryogenic trap to concentrate condensable product species for several hours (Figure 3). The background of the cryogenic

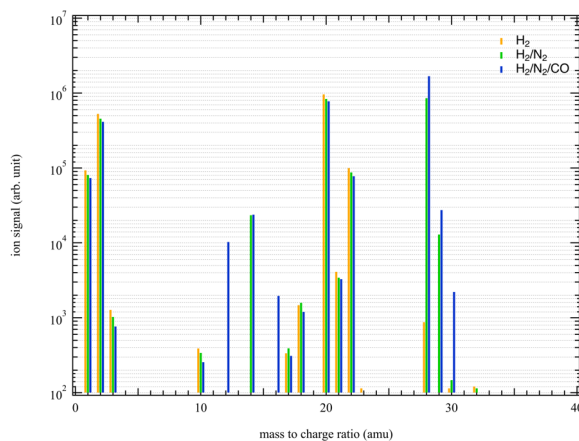


Fig. 2. Experimental mass spectra of neutral species obtained *in situ* with a H_2 (orange bars), $\text{H}_2\text{-N}_2$ (green bars), and $\text{H}_2\text{-CO-N}_2$ (blue bars) gas mixtures irradiated in the APSIS photochemical reactor at 73.6 nm.

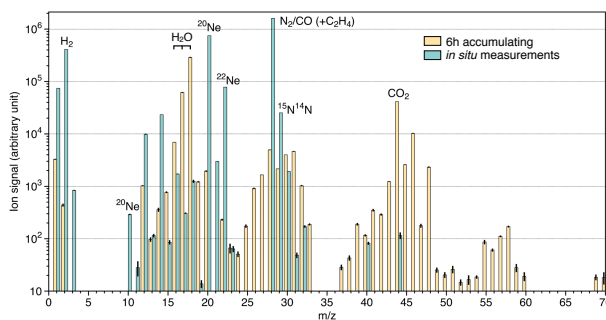


Fig. 3. Experimental mass spectra of neutral species obtained *in situ* (light blue) and after 6 hours of accumulation in a cryogenic trap (yellow), with a $\text{H}_2\text{-CO-N}_2$ gas mixture irradiated in the APSIS photochemical reactor at 73.6 nm. Standard deviation (in 10 measurements of each mass) is displayed.

trap was controlled to be negligible by carrying out an experiment without irradiation. The same gas flow was injected continuously in the reactor (same pressure conditions) including neon from the photon source side. However the discharge of the neon gas flow upstream was turned off, thus no photons were produced leading to a non-reactive experiment without photochemistry (Figure 4). This demonstrate that molecules assumed to be formed after irradiation are not present without irradiation. In addition, the level of water contamination which is the major pollutant were measured in the reactor at trace level (cf. Figure 2). The organic contaminants possibly present in the neon gas bottle have a total molar fraction below 10^{-7} , so 6 to 7 orders of magnitudes lower than CO, the chosen source of carbon in our case. Finally if contaminants were here and could contribute largely to the formation of the new species detected in the green mass spectrum, then their own concentration would decrease through the irradiation process compared to the blank experiment. This is not what we observe in Figure 4 : no organic molecule that could be in the yellow spectrum (blank) decreases compared to the green spectrum (experiment): neither in the C_2 , nor in the C_3 or C_4 mass block. There is no significant source of organic contaminants seable in the blank that could explain the formation of the new species in the green mass spectrum. Thus, organic photoproducts observed in Figure 4 are coming from CO chemistry.

Also note that the total amount of gas condensed in the cold trap, as estimated from the total pressure in the line after sublimation of the trapped species, was repeatable within ca. 20% in duplicated experiments. Multiplying the trapping duration by a factor 2 yielded a total gas pressure being also increased by a factor 2 (here, 0.05 mbar for 3 hours and 0.1 mbar for 6 hours). On the mass spectrum in Figure 4, corresponding to 3 hours of accumulation in the cryogenic trap, we note the presence of blocks at m/z around 24-32 (so-called C_2), 38-48 (so-called C_3) and 51-60 (so-called C_4). These blocks correspond to the ion fragments of the stable neutral molecules released by the cold trap (fragmentation pattern FP of the electron impact at 70 eV in the ionization chamber of the mass spectrometer). In the first block, we observe the formation of small C_2 -hydrocarbons C_2H_2 (FP at m/z 24, 25 and 26) and C_2H_4 (FP at m/z 26, 27 and 28). HCN is suspected but cannot be confirmed as its FP at m/z 26, 27 overlaps with ethylene. Ethane C_2H_6 might also be produced but is hardly distinguishable with its main overlapping FP at m/z 27, 28.

Additional peaks at m/z of 29, 30 and 31 might be attributed to several molecules. The importance of the ion intensity at m/z 31 is consistent with the major ion of the fragmentation pattern of methanol CH_3OH (FP at m/z 31, 32). Likewise, the high contribution of ions at m/z 30 is probably the indicator of nitrogen monoxide NO, but a contribution from methylamine CH_3NH_2 cannot be ruled out (FP at m/z 30, 31 with a major ion at m/z 30). The peak at m/z 29 could be attributed to the main FP of formaldehyde H_2CO and/or methanimine CH_2NH . Uncertainties associated with the identification of molecules invariably increase with increasing mass, given that more and more candidate species could contribute altogether and deconvoluting their associated signals is not straightforward.

It should be noted that NO and C_2H_4 mostly desorb at 40 and 50 K respectively (Collings et al. 2004). However the desorption proceeds up to 80 K for both compounds, thus the desorption of NO and C_2H_4 even very limited is still present at 77 K.

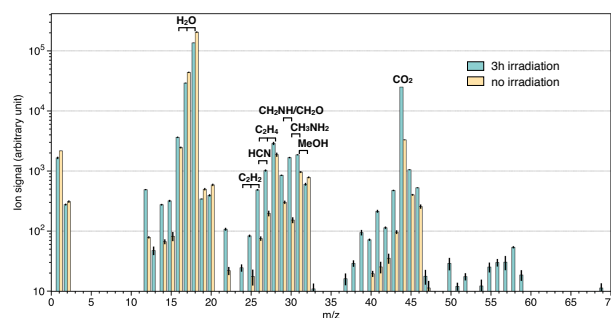


Fig. 4. Experimental mass spectra obtained for neutral species with a H₂-CO-N₂ gas mixture with (light blue) and without (yellow) irradiation in the APSIS chamber by using a 3h cryogenic trapping system. Standard deviation (in 10 measurements of each mass) is displayed.

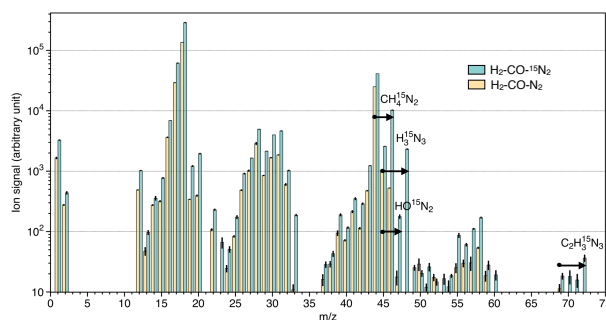


Fig. 5. Experimental mass spectra obtained for neutral species with an isotopically labeled H₂-CO-¹⁵N₂ (yellow) and H₂-CO-N₂ gas mixture (light blue), irradiated in the APSIS photochemical reactor at 73.6 nm by using a 3h cryogenic trapping system. Standard deviation (in 10 measurements of each mass) is displayed. The arrows indicate the shift in masses when using the isotopically marked mixture.

We therefore performed additional experiments under the same conditions but with an isotopically labeled gas mixture (H₂-CO-¹⁵N₂; Figure 5). Comparing mass spectra obtained for neutral species for H₂-CO-N₂ and H₂-CO-¹⁵N₂ indicates a shift of peaks at m/z of 33, 46, 47 and 48, revealing these mainly correspond to N-bearing species. The appearance of a peak at m/z of 33 can be attributed to the presence of ¹⁵N₂H₃⁺ (shift from m/z 31), which could be a fragment of stable molecules detected at higher masses such as methyldiazene (CH₃-N=NH m/z 44) and triazene (NH₂-N=NH m/z 45). Those molecules are indeed identified in the C₃ block thanks to the isotopic labeling, with the appearance of signatures at m/z 46 (CH₄¹⁵N₂) and m/z 48 (H₃¹⁵N₃). The ion at m/z 47 is consistent with the signature of ¹⁵NO₂. In the C₄ block, a decrease of the contribution at m/z 56 reveals the presence of a nitrogen-containing species, shifting to higher masses with the isotopic labeling, but unequivocally attributing this shift to the presence of a given molecule is hampered by contributions from other molecules at m/z 57, 58 and 59. Finally in the C₅ block, the only detectable contribution without labeling at m/z 69 is clearly shifted to m/z 72, enabling to identify the corresponding molecule: triazole C₂H₃N₃. This aromatic structure has several possible isomers, with two or three adjacent nitrogen atoms in the cycle. The detection of triazene and acetylene could explain the formation of triazole isomers heterocyclic compounds (Totobenazara & Burke 2015).

Table 1 reports potential neutral species detected in this work compared to molecules in CSEs up to the detected mass range analysed in this work. We discuss below the similarities and differences with observations.

Methanimine and methylamine were both observed as gas-phase interstellar molecules and thought as potential interstellar precursors to the amino acid glycine (NH₂CH₂COOH) (Theulé et al. 2011; Danger et al. 2011). CH₂NH was found in every environment in nearly every environment, but critical production pathways are still lacking. Gas-phase reactions such as CH + NH₃ (Tenenbaum et al. 2010) or photolysis from CH₃NH₂ (Michael & Noyes 1963) have been proposed to explain the observed fractional abundances of methanimine. However, the formation rates are too low and alternative sources in condensed matters have been proposed, such as sequential hydrogenation of HCN on grain surfaces producing both methylamine and methanimine (Halfen et al. 2013). The potential detection of both species in this grain-free work would support the fact that there is still missing formation pathways in the gas-phase. Since ammonia has not been detected in this work, the reaction between NH₃ and CH radicals is unlikely and other bimolecular neutral-neutral reactions should be considered such as N(²D) + CH₄ (Yelle et al. 2010).

Two compounds have been found in abundance in our experiment: formaldehyde H₂CO and methanol CH₃OH. Methanol, a precursor of complex organic molecules potentially leading to amino acids and other astrobiologically relevant species (Öberg et al. 2009), has been detected in both solid and gas phases in molecular clouds and protostellar envelopes (Graninger et al. 2016; Lee et al. 2017; Olofsson et al. 2017). However, as for methanimine, the abundance of CH₃OH has not been reproduced by orders of magnitude using a pure gas-phase chemical network (Geppert et al. 2006; Garrod et al. 2006), and gas-grain models are used with a preponderance of hydrogenation reactions (Theulé et al. 2011). Thus, methanol is thought to be mainly produced through hydrogenation of CO, including few intermediates such as HCO, H₂CO and CH₂OH (Garrod et al. 2007). Formaldehyde is known to be produced through the same formation pathways on grain surfaces along with efficient gas phase formation via the reactions O + CH₃ and OH + CH₂ (Ford et al. 2004). This work addresses the formation of methanol and formaldehyde following ion-driven gas phase reactions. Even if mass spectrometry does not provide accurate quantification, relative production rates can be estimated

Table 1. Potential neutral species detected in this work compared to molecules detected in CSEs. A dash in the second column refers to non-detection.

Experiments	Observations in CSEs
C ₂ H ₂	C ₂ H ₂
HCN	HCN
C ₂ H ₄	C ₂ H ₄
CH ₂ NH	CH ₂ NH
H ₂ CO	H ₂ CO
CH ₃ NH ₂	–
NO	NO
CH ₃ OH	CH ₃ OH
CO ₂	CO ₂
CH ₃ N ₂ H	–
N ₃ H ₃	–
NO ₂	–
C ₂ H ₃ N ₃	–

based on the ion intensity of the main fragments at m/z 29 and 30. The methanol-to-formaldehyde ratio appears to be close to one, which is lower than expected in interstellar environments, therefore indicating a points out a more efficient gas-phase pathway to form H₂CO under oxidative conditions (Atkinson et al. 2006).

Among the several N-bearing species that have been detected in circumstellar environments, none of them contains oxygen except nitrile oxide NO (Quintana-Lacaci et al. 2013). Even if nitric oxides act as a N-reservoir and as precursors for the production of complex molecules, many of them such as NO₂ have not yet been detected in CSEs. NO is a key intermediate molecule in the ISM leading to the formation of nitrogen hydrides and nitriles (Le Gal et al. 2014), and the detection of NO in this work supports the chemical relationship between HCN and NO, as already displayed by modeling of the chemistry in astrophysical environments (Li et al. 2016)

The isotopically labelled gas mixture analysis reveals the presence of methyldiazene CH₄¹⁵N₂ and triazene H₃¹⁵N₃. Methyldiazene has been detected as a product of the photo-desorption of H₂O:CO:NH₃ circumstellar ice analogues (Jimenez-Escobar et al. 2018) and triazene has also been observed as a product in the gas phase of ammonia-bearing ice irradiation (Förstel et al. 2016). Those N-bearing molecules are potential precursors that would explain the formation of interstellar triazole C₂H₃N₃. One formation pathway for this aromatic structure could be a Huisgen’s cycloaddition reaction between an azide and an aldehyde or alkyde, thus matching with the detection of triazene and acetylene or formaldehyde in the reactor (Totobenazara & Burke 2015). Our work therefore supports a photochemical reaction pathway toward the formation of N-containing heterocyclic aromatic compounds (N-heterocycles) in CSEs, and more generally in space. Even if the last decade has seen considerable progress in understanding the reactions leading to the formation of polycyclic aromatic hydrocarbons (PAHs), little is known about the synthesis of N-containing PAHs, which are considered as precursors of biorelevant molecules such as nucleobases (Peeters et al. 2003). This work lends credence to models of photochemical reactions from simple species to monocyclic systems toward the formation of NPAHs in CSEs and, more genererally, in the ISM.

3.2. Ions

In situ gas-phase mass spectra of ionic species with H₂-CO-N₂ irradiated at 73.6 nm displayed in Figure 6 comprise main peaks at m/z of 1, 2, 3, 18, 19, 28, 29, 37, 45, 47 and 57. The peaks at m/z of 1, 2 and 3 are attributed to the presence of H⁺, H₂⁺ and H₃⁺, respectively, whereas m/z of 18, 19 and 37 correspond to chemical derivatives of water with H₂O⁺, H₃O⁺ and H₂O(H₃O⁺), respectively. Thus, these ions must also be formed in the CSEs since there is water vapour. Using the same isotopic labelled gas mixture as reported Figure 5, we identify N₂H⁺ and HCO⁺, both detected at m/z of 29, with a rise in the signal at m/z of 31 (20 times lower than the signal at m/z 28) being attributed to N₂H⁺ in the case of a H₂-CO-¹⁵N₂ gas mixture (Figure 6). Finally, peaks at m/z of 45, 47 and 57 could correspond to several species, including HCO₂⁺/HON₂⁺/C₂H₅O⁺, C₂H₇O⁺ and C₄H₉⁺/C₃H₅O⁺, respectively.

Table 2 reports potential ionic species detected in this work compared to ions detected in CSEs. The lightest ionic molecules detected in this work are the abundant H⁺, H₂⁺ and H₃⁺. Even if chemical processes in the ISM involve efficient molecular ion reactions, especially in photodissociation regions, simpler molecular ions such as H⁺ and H₂⁺ have still not been detected due to the lack of associated dipole moment, making infrared and radio frequency detections extremely challenging. Only H₃⁺ has so far been detected in interstellar space (Geballe & Oka 1996). It has notably been proposed to form by the reaction between H₂ and H₂⁺, which is also the most likely process accounting for its measurement in the APSIS reactor.

In the present study, we did not detect CH⁺ whereas it has been detected in CSEs (Table 2). This is probably due to the too small amounts of hydrocarbons being present in the reactor, given that no hydrocarbons such as CH₄ or C₂H₂ were introduced as initial species. In the same way, we are not able to differentiate if the signal at m/z of 15 corresponds to CH₃⁺ or NH⁺, even using isotopic labelled gas mixture due to important fragmentation products of residual water in the mass spectrometer at m/z 16 and 17. However, we observe a decrease by a factor of 2 from the signal at m/z 17 by switching N₂-mixture with ¹⁵N₂-mixture meaning that a significant proportion of NH₃⁺ has been formed through the H₂O⁺ + NH₂ reaction.

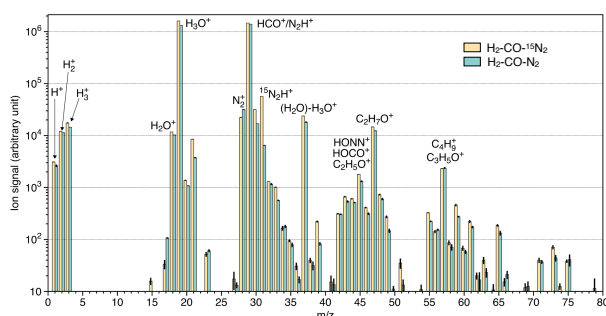


Fig. 6. Experimental mass spectra obtained for ionic species with an isotopic labelled H₂-CO-¹⁵N₂ (yellow) and a H₂-CO-N₂ gas mixture (light blue) irradiated in the APSIS chamber. Standard deviation (in 10 measurements of each mass) is displayed.

Table 2. Potential ionic species detected in this work compared to molecules detected in CSEs. The lines in the third column refers to non detection.

Experiments	Observations
H ⁺	—
H ₂ ⁺	—
H ₃ ⁺	—
CH ⁺	CH ⁺
CH ₃ ⁺ /NH ⁺	—
OH ⁺ /NH ₃ ⁺	OH ⁺
H ₂ O ⁺	—
H ₃ O ⁺	—
N ₂ ⁺ /CO ⁺	CO ⁺
N ₂ H ⁺ /HCO ⁺	N ₂ H ⁺ /HCO ⁺
C ₂ H ₇ O ⁺	—

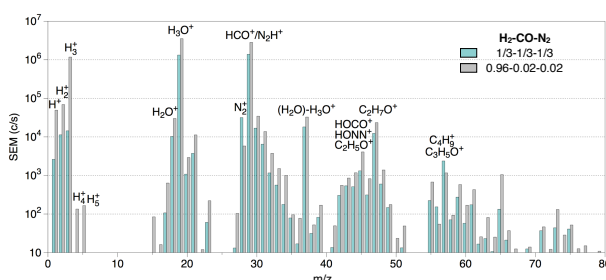


Fig. 7. Experimental mass spectra obtained for ionic species with a 1:1:1 mixing ratio of a H₂-CO-N₂ gas mixture (light blue) and a 1:0.01:0.01 mixing ratio of a H₂-CO-N₂ gas mixture (gray) irradiated in the APSIS chamber.

Chemical derivatives of water with H₂O⁺ and H₃O⁺ are detected among the main ions in Figure 6. As explained and shown before (cf. Figure 2), water H₂O is the main pollutant in the reactor and CO⁺ is one of the primary ions formed by the photolysis of CO. Thus, HCO⁺ is easily formed through the reaction between CO⁺ and H₂. Once formed the proton-transfer reaction with water leads to the formation of H₃O⁺, which is a side product. However, its formation does not affect the overall chemistry and acts as proton-donor agent like HCO⁺.

We definitely form CO⁺ and N₂⁺ at m/z of 28 since we observe a shift from m/z of 28 to m/z of 30 by using the isotopic labelled gas mixture, matching with the presence of ¹⁵N₂⁺. In the same way, we observe HCO⁺ and ¹⁵N₂H⁺ at m/z of 29 and 31, respectively. Due to the specificity of the experiments regarding the simplified gas mixture, HCO⁺ is likely coming from CO⁺, produced by photoionization of CO and reaction with H₂, rather than from H₃⁺ + CO or C⁺ originating from the dissociative ionization of CO, as thought in CSEs (Li et al. 2016). Following the same thought, N₂H⁺ is likely formed via the reaction N₂⁺ + H₂ rather than from H₃⁺ + N₂. It is produced in much smaller quantity than HCO⁺, as seen in the signal at m/z 31 being ca. 20 times lower than that of HCO⁺ at m/z 29. This is unexpected based on similar absorption cross section for N₂ and CO at the wavelength used in this work and similar coefficient rates between N₂⁺ and CO⁺ with H₂ (Scott et al. 1997; Adams et al. 1980).

Heavier ions were also detected up to m/z 80, but their identification is challenging. Signals at m/z 47 and 57 could be attributed to C₂H₇O⁺, formed through H₃O⁺ + C₂H₄ (Fairley et al. 1997), and C₃H₅O⁺. One of the major findings of the present work is that, even with a simple starting gas mixture such as H₂-CO-N₂, heavier ions containing few N-, O- and C-atoms could be formed.

As mentioned in the experimental method section, a gas mixture with a H₂-CO-N₂ mixing ratio 1:0.01:0.01 was used to mimic a H-dominated environment. Figure 7 compares experimental mass spectra obtained for ionic species with the 1:1:1 mixing ratio

of a H₂-CO-N₂ gas mixture and the H-dominated gas mixture, irradiated in the APSIS chamber. This result allows us to probe the evolution of the ionic species distribution as function of the mixing ratio of H₂. It demonstrates that even with 100 times more hydrogen, the formation and/or consumption of the species do not seem to be significantly affected, with only the respective distribution varies.

In a H₂-dominated environment, photoionization leads to the formation of H₃⁺ mainly through the well-known H₂⁺ + H₂ reaction. Once formed it leads to the formation of HCO⁺ and N₂H⁺ through the reactions H₃⁺ + CO and H₃⁺ + N₂ respectively. In the case of the low H₂ environment, the primary ions N₂⁺ and CO⁺ formed at 73.6 nm trigger the molecular growth reacting with H₂, leading to the formation of HCO⁺ and N₂H⁺. As a conclusion the results show that the same main ions should be observed in poor and H₂-rich environments like in those experiments. However, they are formed through different chemical pathways by H-transfer reactions leading to the observed stable protonated ions. These results highlight the need to accurately model ion-neutral chemistry in photon-dominated environments. Thus, the abundance of species does not depend on the initial ratio because they give the same main abundant ions in the reactor but through different formation pathways. This comparison further supports the suitability of the photochemical cell for experimentally mimicking processes involved in the molecular growth scheme within outer CSEs.

4. Conclusions

1. Taken together, our data indicate that photochemical reactions occurring within the APSIS reactor from H₂-CO-N₂ gas mixtures are relevant to simulate processes of molecular growth within the irradiated, outermost regions of CSEs. We find the dominant products of photochemical reactions between CO, N₂ and H₂ to be N₂H⁺, and most importantly HCO⁺, which has been widely observed within CSE environments. Molecular ions are known to play a significant role in building up the molecular complexity observed within, e.g., the interstellar medium, PDRs, dark clouds, and star-forming regions. However, their detection in (post-)AGB stars or planetary nebula remains limited to simple ions (HCO⁺, N₂H⁺, CO⁺, NH⁺, CH⁺, OH⁺; see, e.g., Zhang et al. (2008); Pardo et al. (2007); Aleman et al. (2014)). In our experiment, heavier molecular ions have also been detected, but their identification is challenging. Nevertheless, their presence in our experiment witnesses that complex ion-molecule chemistry is at stake within stellar environments, possibly as a result of photochemical reactions starting from simple molecules (H₂, CO and N₂) in the gas phase.
2. Some of the neutral species detected in our experimental setup have been observed in the circumstellar medium, e.g. small C₂ hydrocarbons such as C₂H₂ and C₂H₄, oxygenated molecules with methanol CH₃OH and formaldehyde H₂CO, and the first N-bearing molecules HCN and CH₂NH. Additionally, we detected complex nitrogenized species: methylamine CH₃NH₂, methyl diazene CH₄N₂, triazene N₃H₃, and a heteroaromatic structure triazole C₂H₃N₃, which have not yet been observed around evolved stars and could therefore potentially be searched for. It is worth noting that some of the species observed within our experiments have already been observed during photo-desorption experiments of circumstellar ice analogues. Regarding the ionic species, we detect less species at high molecular weight than has been observed in the circumstellar medium. This could be explained by the fact that CO and N₂ are the only parent species used in our experiments, whereas HCN, C₂H₂ and NH₃ would for instance be present in CSEs (Figure 1). These are notably taken into account as parent species in chemical kinetic models used to simulate CSE environments (e.g., Li et al. (2014, 2016)). Thus, although we observe ionic species up to m/z 80, molecular growth is probably hindered in our experimental setting and future experiments should therefore consider using more complex parent species.
3. Importantly, we observe that photons at 73.6 nm induce the formation of dominant ions observed in CSEs (N₂H⁺, HCO⁺). This suggests that EUV experiments < 100 nm akin to the present experimental setting or synchrotron facilities, allow reproducing chemical processes occurring within outer CSEs. Additional experiments should further consider using the tunability of synchrotron radiation to undertake a multi-wavelength approach and reach the (dissociative) ionization regime of the different species for more complex gas mixtures including parent species formed in the inner CSEs (e.g., NH₃, HCN, C₂H₂). This should ultimately allow inferring their role in molecular growth processes during stellar evolution, and reach the molecular diversity observed in the circumstellar medium with the detection of heavy exotic chemical species, including unsaturated long-chain hydrocarbon such as polyynes (HC₅N, HC₇N, HC₉N) (Brotten et al. 1978; Winnemissner & Walmsley 1978). Future experiments might also focus on the detection of molecular anions, which have only been found to our knowledge in one circumstellar object (e.g., Cernicharo et al. (2007); Agúndez et al. (2010)).
4. In this work, we identify important potential species such as heteroaromatic N-compound triazole, suggesting N-based roots towards the formation of N-aromatic compounds in circumstellar environments, that could orientate future observational investigations of CSEs chemical products. Furthermore, the suitability of our photochemical cell for experimentally mimicking processes involved in the first stages of molecular growth within outer CSEs opens a new avenue of experimental investigations based on simple species such as acetylene, methylamine, methanimine and formaldehyde, for better understanding the complex pathways of fundamental reaction mechanisms within circumstellar environments. These experiments would also provide important information to explain the effects of UV radiation and fundamental reaction mechanism on the molecular growth scheme in the ISM.

Acknowledgements. This research was supported by the European Research Council Starting Grant PRIMCHEM 636829 to N.C. and the European Research Council Grant PHOTONIS 695618 to B.M.

References

- Adams, N. G., Smith, D., & Paulson, J. F. 1980, *The Journal of Chemical Physics*, 72, 288
 Agúndez, M., Cernicharo, J., Guélin, M., et al. 2010, *Astronomy & Astrophysics*, 517, L2

- Agúndez, M., Cernicharo, J., Quintana-Lacaci, G., et al. 2017, *Astronomy & Astrophysics*, 601, A4
- Agúndez, M., Fonfría, J., Cernicharo, J., et al. 2012, *Astronomy & Astrophysics*, 543, A48
- Aleman, I., Ueta, T., Ladjal, D., et al. 2014, *Astronomy & Astrophysics*, 566, A79
- Atkinson, R., Baulch, D., Cox, R., et al. 2006, *Atmospheric Chemistry and Physics*, 6, 3625
- Bourgalais, J., Carrasco, N., Vettier, L., & Pernot, P. 2019, *Journal of Geophysical Research: Space Physics*, DOI: 10.1029/2019JA026953
- Brotten, N., Oka, T., Avery, L., MacLeod, J., & Kroto, H. 1978, *The Astrophysical Journal*, 223, L105
- Carrasco, N., Giuliani, A., Correia, J.-J., & Cernogora, G. 2013, *Journal of synchrotron radiation*, 20, 587
- Carrasco, N., Hébrard, E., Banaszekiewicz, M., Dobrijevic, M., & Pernot, P. 2007, *Icarus*, 192, 519
- Cernicharo, J., Guélin, M., Agúndez, M., et al. 2007, *Astronomy & Astrophysics*, 467, L37
- Collings, M. P., Anderson, M. A., Chen, R., et al. 2004, *Monthly Notices of the Royal Astronomical Society*, 354, 1133
- Danger, G., Borget, F., Chomat, M., et al. 2011, *Astronomy & Astrophysics*, 535, A47
- Decin, L., Justtanont, K., De Beck, E., et al. 2010, *Astronomy & Astrophysics*, 521, L4
- Dubois, D., Carrasco, N., Bourgalais, J., et al. 2019, *The Astrophysical Journal Letters*, 872, L31
- Fairley, D. A., Scott, G. B., Freeman, C. G., MacLagan, R. G., & McEwan, M. J. 1997, *The Journal of Physical Chemistry A*, 101, 2848
- Ford, K. S., Neufeld, D. A., Schilke, P., & Melnick, G. J. 2004, *The Astrophysical Journal*, 614, 990
- Förstel, M., Tsegaw, Y. A., Maksyutenko, P., et al. 2016, *ChemPhysChem*, 17, 2726
- Garrod, R., Park, I. H., Caselli, P., & Herbst, E. 2006, *Faraday Discussions*, 133, 51
- Garrod, R. T., Wakelam, V., & Herbst, E. 2007, *Astronomy & Astrophysics*, 467, 1103
- Gautier, T., Carrasco, N., Buch, A., et al. 2011, *Icarus*, 213, 625
- Geballe, T. & Oka, T. 1996, *Nature*, 384, 334
- Geppert, W. D., Hamberg, M., Thomas, R. D., et al. 2006, *Faraday discussions*, 133, 177
- Gobrecht, D., Cherkneff, I., Sarangi, A., Plane, J., & Bromley, S. 2016, *Astronomy & Astrophysics*, 585, A6
- González-Alfonso, E. & Cernicharo, J. 1999, *The Astrophysical Journal*, 525, 845
- González-Alfonso, E., Cernicharo, J., Alcolea, J., & Orlandi, M. 1998, *Astronomy and Astrophysics*, 334, 1016
- Graninger, D. M., Wilkins, O. H., & Öberg, K. I. 2016, *The Astrophysical Journal*, 819, 140
- Habing, H. 1968, *Bulletin of the Astronomical Institutes of the Netherlands*, 19, 421
- Halfen, D., Ilyushin, V., & Ziurys, L. M. 2013, *The Astrophysical Journal*, 767, 66
- Hébrard, E., Dobrijevic, M., Pernot, P., et al. 2009, *The Journal of Physical Chemistry A*, 113, 11227
- Ilgner, M. & Nelson, R. P. 2006, *Astronomy & Astrophysics*, 445, 205
- Jimenez-Escobar, A., Ciaravella, A., Cecchi-Pestellini, C., et al. 2018, arXiv preprint arXiv:1810.03302
- Le Gal, R., Hily-Blant, P., Faure, A., et al. 2014, *Astronomy & Astrophysics*, 562, A83
- Lee, C.-F., Li, Z.-Y., Ho, P. T., et al. 2017, *The Astrophysical Journal*, 843, 27
- Li, X., Heays, A. N., Visser, R., et al. 2013, *Astronomy & Astrophysics*, 555, A14
- Li, X., Millar, T. J., Heays, A. N., et al. 2016, *Astronomy & Astrophysics*, 588, A4
- Li, X., Millar, T. J., Walsh, C., Heays, A. N., & Van Dishoeck, E. F. 2014, *Astronomy & Astrophysics*, 568, A111
- Maercker, M., Schöier, F. L., Olofsson, H., et al. 2009, *Astronomy & Astrophysics*, 494, 243
- Michael, J. V. & Noyes, W. A. 1963, *Journal of the American Chemical Society*, 85, 1228
- Neufeld, D., González-Alfonso, E., Melnick, G., et al. 2011, *The Astrophysical Journal Letters*, 727, L29
- Öberg, K. I., Garrod, R. T., Van Dishoeck, E. F., & Linnartz, H. 2009, *Astronomy & Astrophysics*, 504, 891
- Olofsson, H., Vlemmings, W., Bergman, P., et al. 2017, *Astronomy & Astrophysics*, 603, L2
- Pardo, J. R., Cernicharo, J., Goicoechea, J. R., Guélin, M., & Ramos, A. A. 2007, *The Astrophysical Journal*, 661, 250
- Peeters, Z., Botta, O., Charnley, S., Ruitkamp, R., & Ehrenfreund, P. 2003, *The Astrophysical Journal Letters*, 593, L129
- Peng, Z., Gautier, T., Carrasco, N., et al. 2013, *Journal of Geophysical Research: Planets*, 118, 778
- Quintana-Lacaci, G., Agúndez, M., Cernicharo, J., et al. 2013, *Astronomy & Astrophysics*, 560, L2
- Scott, G. B., Fairley, D. A., Freeman, C. G., et al. 1997, *The Journal of chemical physics*, 106, 3982
- Tenenbaum, E., Dodd, J., Milam, S., Woolf, N., & Ziurys, L. M. 2010, *The Astrophysical Journal Letters*, 720, L102
- Theulé, P., Borget, F., Mispelaer, F., et al. 2011, *Astronomy & Astrophysics*, 534, A64
- Tielens, A. G. 2005, *The physics and chemistry of the interstellar medium* (Cambridge University Press)
- Tigrine, S., Carrasco, N., Vettier, L., & Cernogora, G. 2016, *Journal of Physics D: Applied Physics*, 49, 395202
- Totobenazara, J. & Burke, A. J. 2015, *Tetrahedron letters*, 56, 2853
- Van de Sande, M. & Millar, T. 2019, *The Astrophysical Journal*, 873, 36
- Van Dishoeck, E. F. 2014, *Faraday Discussions*, 168, 9
- Winnewisser, G. & Walmsley, C. 1978, *Astronomy and Astrophysics*, 70, L37
- Yelle, R. V., Vuitton, V., Lavvas, P., et al. 2010, *Faraday discussions*, 147, 31
- Zhang, Y., Kwok, S., et al. 2008, *The Astrophysical Journal*, 678, 328